

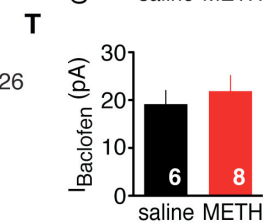
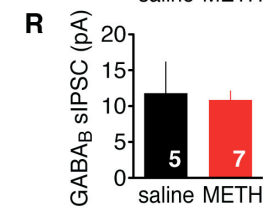
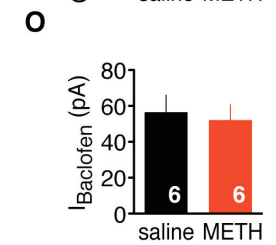
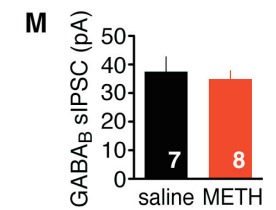
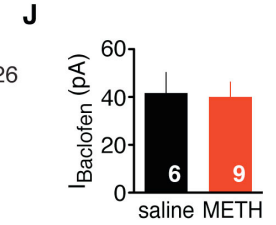
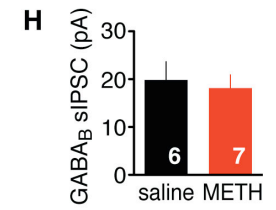
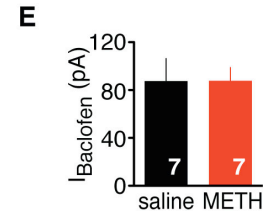
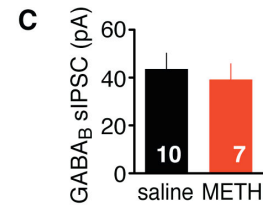
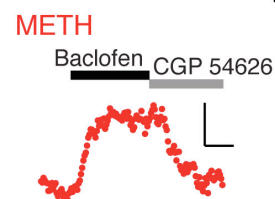
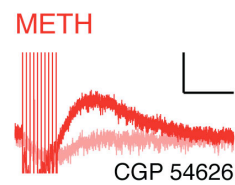
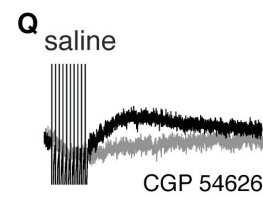
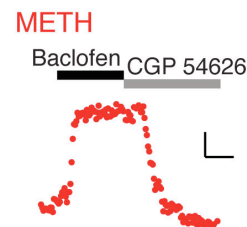
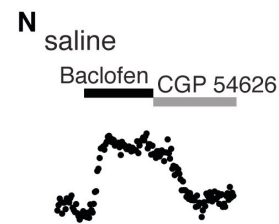
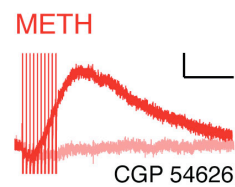
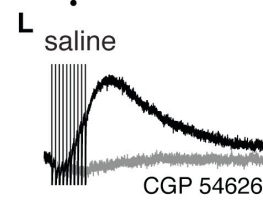
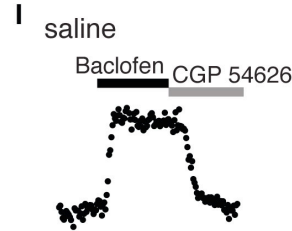
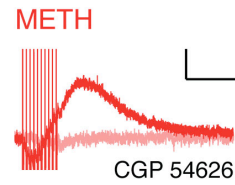
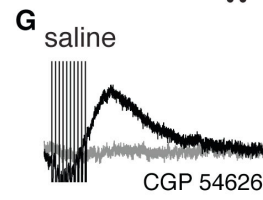
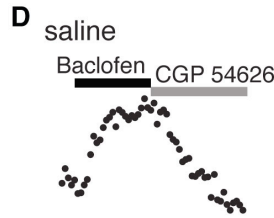
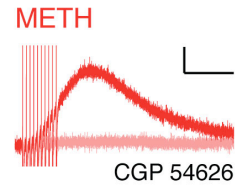
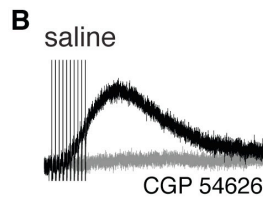
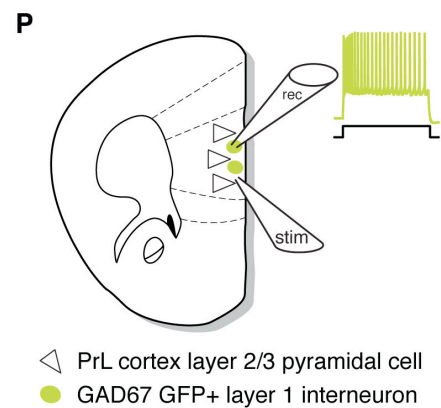
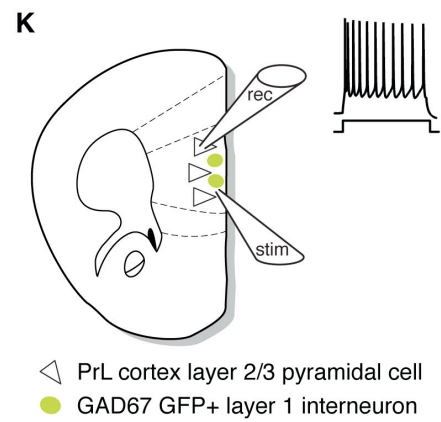
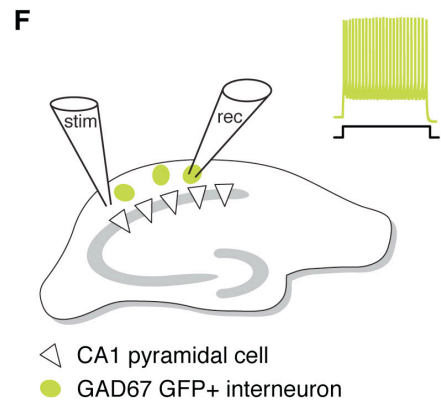
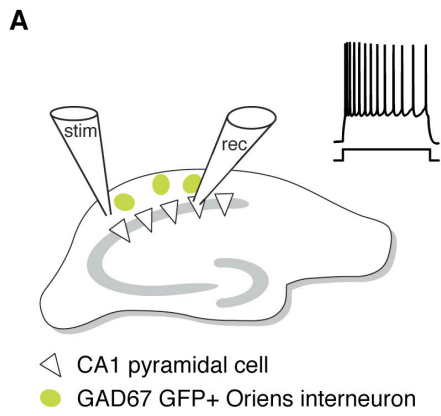
## Supplementary Information

### **Methamphetamine-evoked depression of GABA<sub>B</sub> receptor signaling in GABA neurons of the VTA.**

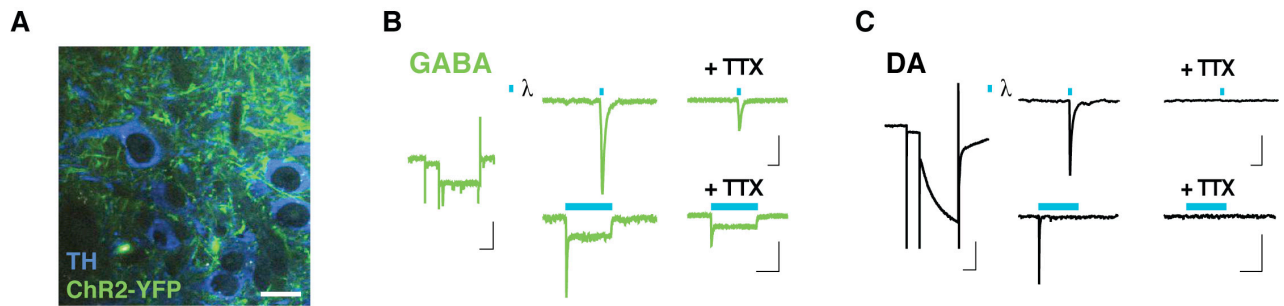
Padgett CL, Lalive AL, Tan KR, Terunuma M, Munoz MB, Pangalos MN, Martínez-Hernández J, Watanabe M, Moss SJ, Luján R, Lüscher C and Slesinger PA

Inventory of supplemental information:

1. Supplemental Figure S1 for Figure 1
2. Supplemental Figure S2 for Figure 3
3. Supplemental Figure S3 for Figure 3
4. Supplemental Methods



**Supplemental Figure S1 (Related to Figure 1). Methamphetamine does not alter GABA<sub>B</sub> receptor signaling in hippocampal and prelimbic cortex neurons.** **A**, Cartoon representing recording of a CA1 pyramidal neuron and stimulation configuration. Inset represents typical firing pattern evoked by a 200pA current step for 500ms. **B**, Example traces of GABA<sub>B</sub>R sIPSC in CA1 pyramidal neurons from saline (black) or METH (red) injected mouse (scale bar: 20pA, 200ms). **C**, Plot of mean amplitude of sIPSC shows no change in METH-injected mice (saline:  $44 \pm 7$  pA, METH :  $39 \pm 7$  pA,  $p > 0.05$ , Mann-Whitney test). **D**, Example recordings of baclofen-evoked currents (300 $\mu$ M) in CA1 pyramidal neurons (scale bar 40pA, 2min). **E**, Plot of average  $I_{\text{Baclofen}}$  shows no change in METH-injected mice (saline:  $88 \pm 19$  pA, METH :  $88 \pm 11$  pA,  $p > 0.05$ , Mann-Whitney test). **F**, Cartoon representing recording of a CA1 Oriens interneuron and stimulation configuration. Inset represents typical firing pattern evoked by a 200pA current step for 500ms. **G**, **H**, Example traces of GABA<sub>B</sub>R sIPSC in CA1 Oriens interneurons from saline (black) or METH (red) injected mice (scale bar: 20pA, 200ms) and average amplitudes (saline:  $20 \pm 4$  pA, METH :  $18 \pm 3$  pA,  $p > 0.05$ , Mann-Whitney test). **I**, **J**, Example recordings of baclofen-evoked currents (300 $\mu$ M) in CA1 Oriens interneurons from saline (black) or METH (red) injected mice (scale bar 20pA, 2min) and average amplitudes (saline:  $42 \pm 7$  pA, METH :  $40 \pm 6$  pA,  $p > 0.05$ , Mann-Whitney test). **K**, Cartoon representing recording of a prelimbic cortex layer 2/3 pyramidal neuron and stimulation configuration. Inset represents typical firing pattern evoked by a 200pA current step for 500ms. **L**, **M**, Example traces of GABA<sub>B</sub>R sIPSC in layer 2/3 pyramidal neurons from saline (black) or METH (red) injected mice (scale bar: 20pA, 200ms) and average amplitudes (saline:  $38 \pm 5$  pA, METH :  $35 \pm 3$  pA,  $p > 0.05$ , Mann-Whitney test). **N**, **O**, Example recordings of baclofen-evoked currents (300 $\mu$ M) in layer 2/3 pyramidal neurons from saline (black) or METH (red) injected mice (scale bar 20pA, 2min) and average amplitudes (saline:  $57 \pm 9$  pA, METH :  $52 \pm 8$  pA,  $p > 0.05$ , Mann-Whitney test). **P**, Cartoon representing recording of a prelimbic cortex layer 1 interneuron and stimulation configuration. Inset represents typical firing pattern evoked by a 200pA current step for 500ms. **Q**, **R**, Example traces of GABA<sub>B</sub>R sIPSC in layer 1 interneurons from saline (black) or METH (red) injected mice (scale bar: 20pA, 200ms) and average amplitudes (saline:  $12 \pm 4$  pA, METH :  $11 \pm 1$  pA,  $p > 0.05$ , Mann-Whitney test). **S**, **T**, Example recordings of baclofen-evoked currents (300 $\mu$ M) in layer 1 interneurons from saline (black) or METH (red) injected mice (scale bar 20pA, 2min) and average amplitudes (saline:  $19 \pm 3$  pA, METH:  $22 \pm 3$  pA,  $p > 0.05$ , Mann-Whitney test). Throughout all experiments cell identity was confirmed by positive or negative GAD67 GFP fluorescence for interneurons and pyramidal neurons respectively, and by firing pattern. Additionally, location of pyramidal neurons in layer 2/3 in the prelimbic cortex was verified by filling the cells with biocytin and CY3 revelation.



**Supplemental Figure S2 (Related to Figure 3). Characterization of blue light-evoked currents in VTA GABA and DA neurons after injecting AAV containing floxed ChR2 into VTA of GAD-Cre mice.** **A**, Expression of ChR2-YFP (green) in the VTA does not colocalize with DA neurons identified by TH staining (blue). **B**, GABA cells were identified by absence of  $I_h$  current (left, scale bar 200pA, 200ms). 3ms light flashes elicited a large current (upper panel, scale bar 100pA, 20ms) that displayed the typical desensitization of ChR2-mediated photocurrent when the light was applied for 400ms (lower panel, scale bar 100pA, 200ms). Additionally, the photocurrent was tetrodotoxin (TTX)-insensitive (the decrease in amplitude is due to the block of synaptic connections among VTA GABA neurons). **C**, DA cells were identified by the presence of a large  $I_h$  current (left, scale bar 200pA, 200ms). 3ms light flashes evoked an action potential-mediated current that was totally blocked by TTX (upper panel, scale bar 100pA, 20ms). No desensitization of the current was observed with prolonged duration of light exposure (lower panel, scale bar 100pA, 200ms).

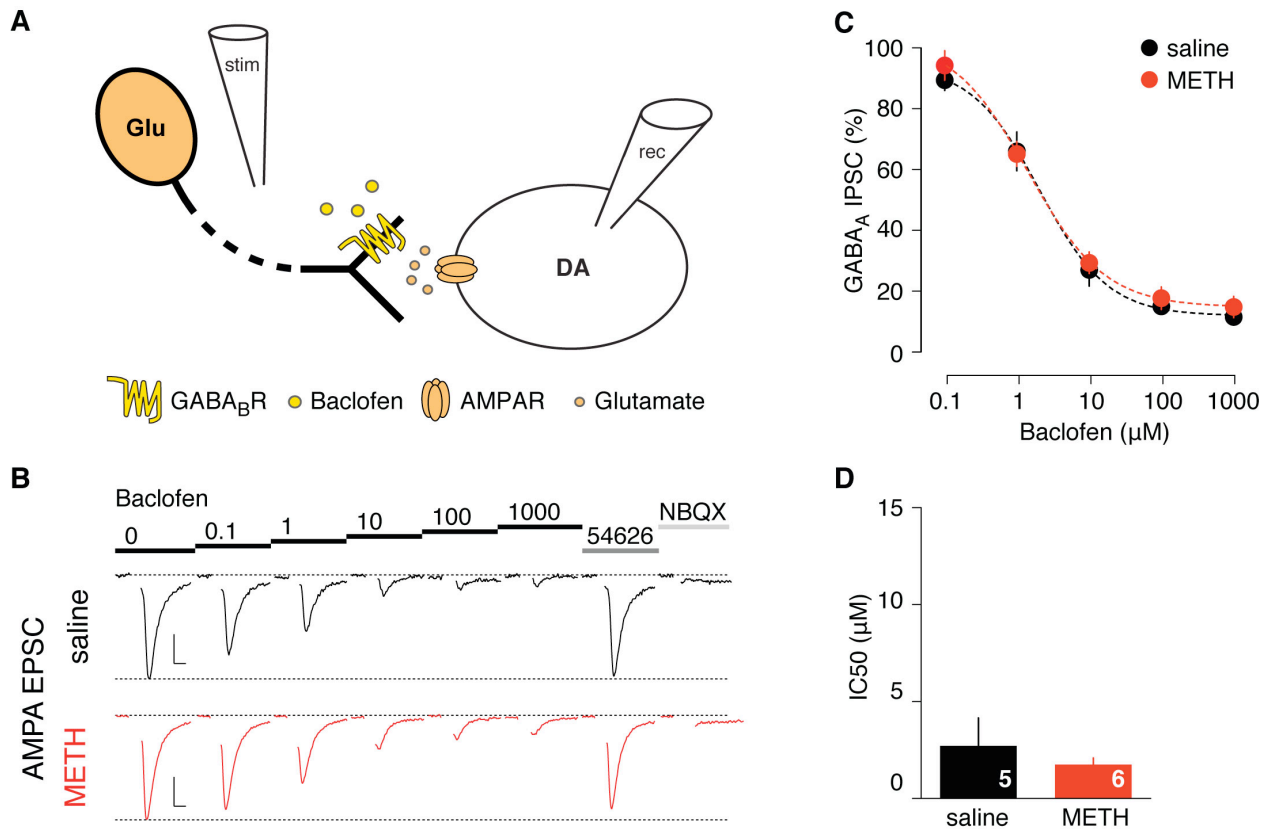


**Figure S3 (Related to Figure 3). GABA<sub>B</sub> receptor-dependent presynaptic inhibition of glutamate onto VTA DA neurons is not altered by METH.** **A**, Schematic showing AMPA EPSC recording from VTA DA neurons evoked by a non-specific electrical stimulation of afferent excitatory fibers. Baclofen impairs glutamate release by acting on presynaptic GABA<sub>B</sub> receptors. **B**, Example traces of electrically evoked EPSCs recorded 24h following saline or METH injection in presence of increasing concentrations of baclofen. Stimulation artifact has been removed for clarity purpose. Basal EPSC amplitude recovers after application of CGP 54626 (2μM) and is subsequently blocked by NBQX (10μM). Scale bars: 50pA, 5ms. **C**, Dose response curves show no difference in sensitivity for baclofen-dependent inhibition of fast IPSCs in METH injected mice after 24h. **D**, Bar graph plots IC<sub>50</sub> for indicated conditions (saline: 2.7 ± 1.4 μM, 24h METH: 1.8 ± 0.3 μM, P < 0.05 Mann-Whitney test).

## Supplementary Methods:

**Electrophysiology in acute slices:** Artificial cerebral spinal fluid (ACSF) contained (in mM) NaCl (119), KCl (2.5), MgCl<sub>2</sub> (1.3), CaCl<sub>2</sub> (2.5), NaH<sub>2</sub>PO<sub>4</sub> (1), NaHCO<sub>3</sub> (26.2) and glucose (11), pH 7.3 continuously bubbled with 95/5% O<sub>2</sub>/CO<sub>2</sub>. Vibratome slices (250µm) were warmed to 33°C and incubated for 45 min in ACSF supplemented with myo-inositol (3), ascorbic acid (0.4) and sodium pyruvate (2) and then transferred to the recording chamber superfused with ACSF (2ml/min).

**Immunoelectron microscopy.** A similar procedure to that described earlier (Luján *et al.*, 1996; Koyrakh *et al.*, 2005) was used. Briefly, free-floating sections were incubated in 10% NGS diluted in TBS for 1 h. Sections were then incubated for 48 h in a mixture of two antibodies (GIRK2 and GAD65/67 or GABAB1 and GAD65/67), at a final protein concentration of 1-2 mg/ml each, diluted in TBS containing 1% NGS. One of the primary antibodies (anti- GAD65/67 antibody) was visualized by the immunoperoxidase reaction and the second one (anti-GIRK2 antibody or anti-GABAB1 antibody) by the silver-intensified immunogold reaction. After primary antibody incubation, the sections were incubated at 4°C overnight in a mixture of the following secondary antibodies: goat anti-rabbit (Fab fragment, diluted 1:100) coupled to 1.4 nm gold (Nanoprobes, Stony Brook, NY), goat anti-guinea pig (Fab fragment, diluted 1:100) coupled to 1.4 nm gold (Nanoprobes, Stony Brook, NY), and biotinylated goat anti-mouse (diluted 1:100; Vector Laboratories) antibodies, all of them made up in TBS containing 1% NGS. After washes in TBS, sections were washed in double-distilled water, followed by silver enhancement of the gold particles with an HQ Silver kit (Nanoprobes, Stony Brook, NY) for 8-10 min. Subsequently, the sections were incubated for 4 hours in the ABC complex (Vector Laboratories) made up in TBS and then washed in TB. Peroxidase was visualized with DAB (0.05% in TB, pH 7.4) using 0.01% H<sub>2</sub>O<sub>2</sub> as substrate for 5-10 min. The sections were washed in PB and then post-fixed with OsO<sub>4</sub> (1% in 0.1 M PB), followed by block-staining with uranyl acetate, dehydration in graded series of ethanol and flat-embedding on glass slides in Durcupan (Fluka) resin. Regions of interest were cut at 70-90 nm thick sections using an ultramicrotome (Reichert Ultracut E, Leica, Austria). Ultrathin sections were mounted on 200-mesh nickel grids. Staining was performed on drops of 1% aqueous uranyl acetate followed by Reynolds's lead citrate. Ultrastructural analyses were performed in a Jeol-1010 electron microscope. Unless otherwise stated, electron microscopic samples were obtained from three different mouse and three blocks of each animal were cut for electron microscopy. To test method specificity of the procedures for electron microscopy, the primary antibody was omitted or replaced with 5% (v/v)

normal serum of the species of the primary antibody. Under these conditions, no selective labelling was observed. In addition, some sections were incubated with both gold-labelled and biotinylated secondary antibodies, followed by the ABC complex and peroxidase reaction without silver intensification. This resulted in amorphous horseradish peroxidase (HRP) end product, and no metal particles were detected. Using the same sequence, but only silver intensification without HRP reaction, resulted in silver grains but no amorphous HRP end product. Under these conditions, only infrequent small patches of HRP end product were detected and the patches were not associated selectively with any particular cellular profile. In addition, the selective location of the signals in structures labelled with only one or the other of the signalling products within the same section, as well as having side by side double-labelled structures, showed that our procedures did not produce false-positive double-labelling results.

**Photomicrograph production.** Electron photomicrographs were captured with CCD camera (Mega View III; Soft Imaging System, Germany). Digitized electron images were then modified for brightness and contrast by using Adobe PhotoShop CS1 (Mountain View, CA) to optimize them for printing.

**Quantitative analysis.** To establish the relative abundance of GIRK2 and GABAB1 immunoreactivity in GABAergic neurons in control conditions and after injection of methamphetamine, quantification of immunolabelling was performed in the VTA from 60  $\mu\text{m}$  coronal slices. For each of three animals, three samples of tissue were obtained (nine total blocks). Electron microscopic serial ultrathin sections were cut close to the surface of each block because immunoreactivity decreased with depth. Randomly selected areas were captured at a final magnification of 50,000X, and measurements covered a total section area of 6000  $\mu\text{m}^2$ . GAD65/67-positive dendritic shafts were assessed for the presence of immunoparticles for GIRK2 or GABAB1. Fifteen dendritic segments were reconstructed for each experimental group from 18 to 25 serial ultrathin sections, using Image J software. The dendritic diameter of individual reconstructed profiles was measured. Linear density of the gold particles in the plasma membrane was obtained by dividing the total number of plasma membrane-bound immunogold particles by plasma membrane length of the reconstructed dendrites. Dendritic surface area was calculated by multiplying the total plasma membrane length of the reconstructed dendrite by the section thickness (70 nm). The total number of plasma membrane-bound gold particles found in the reconstructed dendrite was divided by the dendritic surface area in order to obtain the labelling density of plasma membrane-bound particles in individual profiles.